# Contrast Optimisation of Coherent Images

S. A. Fortune, M. P. Hayes and P. T. Gough
Acoustics Research Group,
Department of Electrical and Computer Engineering,
University of Canterbury,
Private Bag 4800, Christchurch, New Zealand
Email: s.fortune@elec.canterbury.ac.nz

***Abstract*— Contrast optimisation is a method that can be used to correct phase errors in coherent images such as SAS images. However, the contrast measure of a given coherent image is a random variable due to the speckle present in coherent images. The variance of this measure puts a limit on the ability of contrast optimisation to focus an image.**

**This paper derives probability distribution statistics of the most common contrast measure, the sum of the pixel intensities squared. These statistics are then verified by a number of speckle simulations.**

**The developed statistics can be used as a tool to understand and improve the method of contrast optimisation.**

## I. INTRODUCTION

A problem common to many imaging systems is environmental effects causing phase errors to be introduced at the receiver, resulting in blurring of the image. One example is astronomical images suffering degradation due to phase errors introduced by atmospheric turbulence. It is also a major problem in coherent imagery; for example medical ultrasound images are degraded by tissue layers with inhomogeneous acoustic velocities [1], large array radar images are affected by structural flex over time [2], and synthetic aperture radar (SAR) and synthetic aperture sonar (SAS) images are degraded by platform motion [3], [4]. One method for calculating these phase errors in an iterative way is contrast optimisation.

This paper investigates the viability of contrast optimisation to estimate phase errors in coherent images, by investigating the statistics of the contrast measure. The motivation for this work is to apply contrast optimisation to SAS images. The University of Canterbury has developed a sea-going towed SAS, KiwiSAS III. The images and data used in this paper are collected from, or simulated for, this platform.

A major problem with SAS is image degradation caused by platform motion. Any variation in the path of the towfish from a straight line causes unknown phase errors in the recieved data. The synthetic aperture processing coherently combines data from several pings so any phase errors causes severe blurring of the reconstructed image. Applying the correct phase correction to the data removes this blurring. The hope is that the correct towfish path can be estimated by perturbing a set of parameters representing the towfish path so as to maximise the contrast of the reconstructed image. This is the technique of contrast optimisation.

Section II describes the method of contrast optimisation and the variations it can take. Section III develops a model for the statistics of speckle in a coherent image. Using this, the statistical properties of an image contrast measure are derived in Section IV. These statistics are confirmed by simulation results shown in Section V. The effect of the contrast statistics on efforts to maximise the contrast are described in Section VI.

## II. CONTRAST OPTIMISATION

At its most basic, the method of contrast optimisation is to perturb a set of focus parameters so as to maximise an image quality metric of the calculated image. Different contrast optimisation schemes can alter, the set of focus parameters and how they relate to the image, the way image quality is measured, and the method by which the parameters are optimised.

Contrast Optimisation was first used by Muller and Buffington [5] to correct phase distortion in astronomical images. They showed that the simple contrast metric $C = \iint ss(x,y)^2 \mathrm{d}x\,\mathrm{d}y$ where $ss(x,y)$ is the image intensity at point $(x,y)$, is maximum for a correctly focused image. The aperture was divided into segments and a phase correction applied to each segment. The change in image contrast was calculated and used to drive a derivative feedback correction scheme.

Paxman and Marron [6] showed the technique of contrast-optimisation could theoretically be applied to speckled coherent images such as synthetic aperture radar (SAR). Contrast optimisation was then developed for spotlight SAR first by estimating a single motion parameter (acceleration) for a small image [7]. It was also applied to Inverse Synthetic Aperture Radar (ISAR) [8]. It was extended to higher order motions [9] and different contrast measures [10]. For a spotlight system, a closed-form expression can be obtained for the sharpness metric with respect to phase-error parameters. This allows the use of a highly efficient conjugate-gradient search algorithm for the minimisation procedure [11], [12]. Along with this, an arbitrary path, or much higher-order phase errors were estimated. The effect of using various metrics on various image types has been studied [13]. Mostly these methods have shown reasonable results on simulated images, but reliable success on field data has not been displayed.

Due to the more complicated point-spread variant nature of stripmap synthetic aperture imagery, few attempts have been made to use contrast-optimisation autofocus on SAS images [14]. In a method presented by the authors [15] called

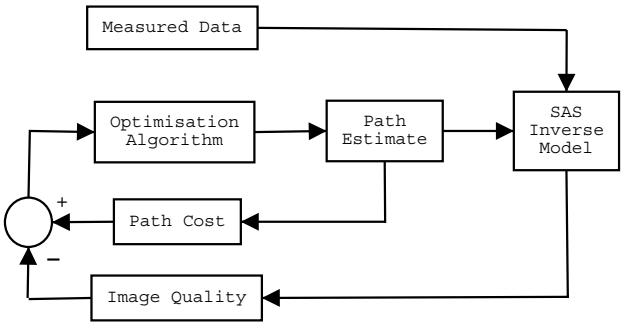


Fig. 1. Overview of statistical autofocus (SAF) method.

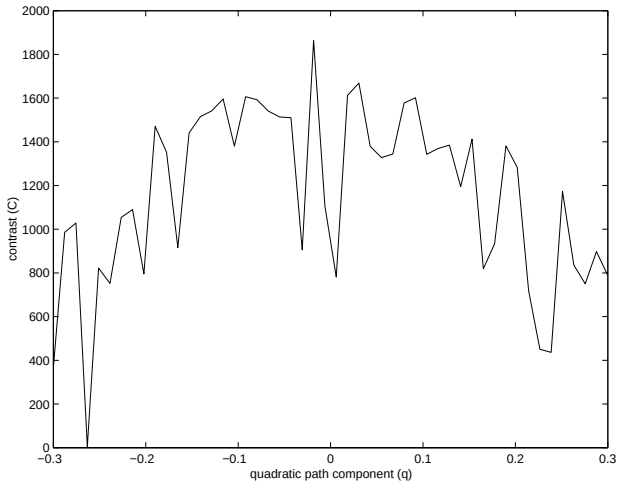


Fig. 2. Variation in contrast as a single focus parameter (quadratic towfish path component) is varied on a field SAS image.

statistical autofocus (SAF), contrast optimisation is presented in a Bayesian framework. This factors in the prior knowledge of the statistics of the towfish motion. The image-quality mesure is a combination of the contrast of the reconstructed image and the log-likelihood of the estimated path. The focus parameters are a set of basis functions optimally representing the towfish path, calculated from the path statistics using the Karhunen-Loeve expansion. The optimisation technique used is a standard multi-variable method, the simplex method of Nelder and Mead [16]. An overview of SAF is shown in Fig. 1.

Although it was an improvement over other methods, SAF still failed when applied to field SAS data. The reason for this became clear when the variation of the contrast measure is mapped as the focus parameters are varied. A typical result of varying a single focus parameter is shown in Fig. 2. Note that this is a cut through a multidimensional space. A local maximum on this cut does not necessarily correspond to a local maximum in multidimensional space. It is, however, a good indicator of the nature of the multidimensional space. Fig. 2 shows the contrast fluctuating in a random manner over an underlying smooth variation which peaks close to zero. The random fluctuation makes it impossible for an optimisation method to find the position of the peak. Section IV explains the reason for this fluctuation and defines some statistics for it.

## III. STATISTICS OF SPECKLE

When a rough surface is illuminated by a coherent source, the scattered field has a granular appearance, as shown in Fig. 3. This is caused by the alternate positive and negative interference of the path from various scatterers and is known as speckle.

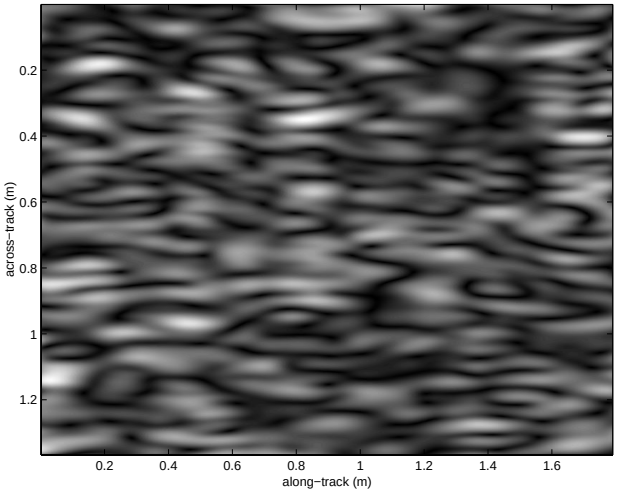


Fig. 3. Example of speckle in SAS intensity image. Across-track bandwidth is double along-track bandwidth.

### A. First-Order Intensity Statistics

Speckle can be modeled by a random walk in the complex plane where each step in the walk is the echo received from a single scatterer [17]. These echos are coherently summed at the receiver and the resultant vector recorded. The intensity $U$ of the resultant field is then a random variable and needs to be dealt with using stochastic methods. For a uniform, sufficiently rough object, the probability density function of the real $(X)$ and imaginary $(Y)$ parts of the field approach a circular Gaussian density function [17] given by

$$\Pr(X,Y) = \frac{1}{2\pi\sigma_X^2}\exp\left(-\frac{X^2+Y^2}{2\sigma_X^2}\right). \tag{1}$$

The speckle intensity $U = X^2+Y^2$ has a negative exponential distribution given by

$$\Pr(U) = \begin{cases} \frac{1}{\sigma_U}\exp\left(-\frac{U}{\sigma_U}\right) & U \geq 0 \\ 0 & \text{otherwise,} \end{cases} \tag{2}$$

where $\sigma_U = 2\sigma_X^2$. The mean and variance of the intensity are given by

$$\mathrm{E}[U] = \sigma_U \tag{3}$$

and

$$\begin{aligned} \mathrm{E}\left[U^2\right] &= 2\,\mathrm{E}[U]^2 \\ \mathrm{Var}[U] &= \mathrm{E}\left[U^2\right] - \mathrm{E}[U]^2 \\ &= \sigma_U^2. \end{aligned} \tag{4}$$

The speckle phase $\theta$ is independent of the intensity and has a uniform distribution given by

$$\Pr(\theta) = \begin{cases} \frac{1}{2\pi} & -\pi \leq \theta < \pi \\ 0 & \text{otherwise.} \end{cases} \quad (5)$$

Note that this distribution applies to an ensemble of single pixel intensities over different speckle realisations.

### *B. Second-Order Intensity Statistics*

Consider the intensity of two separate pixels, $U_1$ and $U_2$, where

$$U_i = X_i^2 + Y_i^2. \quad (6)$$

The correlation between the real and imaginary components of the two pixels is equal and defined as

$$\text{Corr}\left[X_i, X_j\right] = \rho_{ij} \quad (7)$$

and

$$\text{Corr}\left[Y_i, Y_j\right] = \rho_{ij}. \quad (8)$$

The correlation of the intensity of the two pixels can be derived as

$$\begin{aligned} \text{Corr}\left[U_i, U_j\right] &= \frac{\text{E}\left[U_i U_j\right] - \text{E}\left[U_i\right]\text{E}\left[U_j\right]}{\sqrt{\text{Var}\left[U_i\right]\text{Var}\left[U_j\right]}} \\ &= \rho_{ij}^2. \end{aligned} \quad (9)$$

### *C. Non-uniform Object*

Now consider the case of the illumination of a non-uniform diffuse object. Lowenthal and Arsenault [18] showed that the mean intensity of an image pixel is the same as the incoherent image of the same object, with speckle appearing as multiplicitive noise. Using this multiplicitive speckle model, the image intensity can be written as

$$I(m,n) = V(m,n)U(m,n) \quad (10)$$

where $I(m,n)$ is the image intensity at pixel $(m,n)$, $V(m,n)$ is the incoherent image of the object and $U(m,n)$ is the speckle noise. For fully developed, unfiltered speckle, $U(m,n)$ is a random variable with a probability density function given by (2) and $\sigma_U^2 = 1$. In any measured image there is also a component of additive noise, but this is usually much smaller than the speckle noise for a reverberation limited sonar and is ignored in this analysis.

This analysis assumes the speckle noise statistics is constant for all pixels. (It is spatially stationary). The mean of a pixel intensity $I$ does vary with range but this is contained in the incoherent component $V(m,n)$. It is possible to get a reasonable estimate of the statistics of $U$ by looking at a small patch of an image with a constant mean value. For instance, a patch of bland sea-floor with a small range variation. Fig. 4 presents a histogram of the intensity and phase of pixels on a small patch of bland seafloor, showing the expected negative-exponential intensity and uniform phase distributions.

If $U$ is stationary the mean and variance of image intensity $I$ is given by

$$\text{E}\left[I(m,n)\right] = \mu_U V(m,n) \quad (11)$$

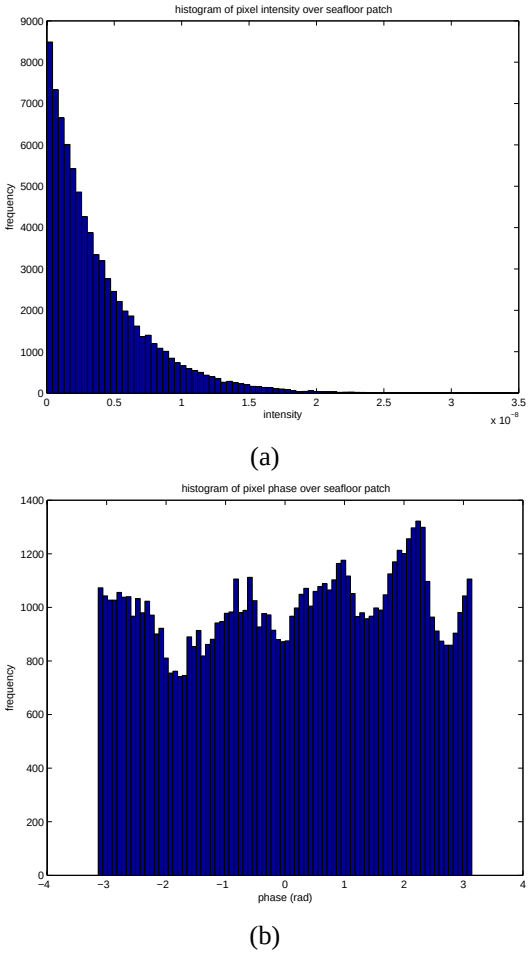


Fig. 4. Histogram of pixels over a patch of seafloor in a field SAS image. (a) pixel intensity, (b) pixel phase.

$$\text{Var}\left[I(m,n)\right] = \sigma_U^2 V^2(m,n), \quad (12)$$

where

$$\mu_U = \text{E}\left[U(m,n)\right]$$

$$\sigma_U^2 = \text{Var}\left[U(m,n)\right].$$

## IV. CONTRAST MEASURE STATISTICS

Let a contrast measure $C$ of the image be the sum of the square of each pixel's intensity, i.e.,

$$C = \frac{1}{N}\sum_{(m,n)} I^2(m,n), \quad (13)$$

where $N$ is the number of pixels summed over.

### *A. Speckle Noise Model*

Using the multiplicative noise model from (10), this can be written as

$$C = \frac{1}{N}\sum_{(m,n)} V^2(m,n)U^2(m,n). \quad (14)$$

Defining the random variable $Z(m,n) \equiv U^2(m,n)$, we get

$$C = \frac{1}{N} \sum_{(m,n)} V^2(m,n) Z(m,n). \tag{15}$$

If the speckle is uncorrelated, $Z(m,n)$ is a set of independent and identically distributed (iid) random variables. Thus $C$ is a sum of iid random variables's, weighted by the non-coherent term $V^2(m,n)$. From the Lindeberg-Feller central limit theorem [19], $C$ will asymptotically approach normal distribution. Fig. 5 compares the results of the contrast of a number of simulated uncorrelated speckle patterns against a normal distribution curve, showing a close match. Fig. 8 shows the effect of increasing speckle correlation on the probability distribution of $C$. It is apparant the probability distribution of the contrast of highly correlated speckle is not normally distributed.

### *B. Negative Exponential Pixel Statistics*

Let us consider fully developed, unfiltered speckle, where $U(m,n)$ has probability distribution given by (2). The probability distribution of $Z$ is given by

$$\Pr(Z) = \begin{cases} \dfrac{1}{2\sigma_U \sqrt{Z}} \exp\left(-\dfrac{\sqrt{Z}}{\sigma_U}\right) & I \geq 0 \\ 0 & \text{otherwise.} \end{cases} \tag{16}$$

The mean of $Z$ is given by

$$\begin{aligned} \mathrm{E}[Z] &= \int_{-\infty}^{\infty} Z \Pr(Z) \mathrm{d}Z \\ &= \int_{0}^{\infty} \frac{\sqrt{Z}}{2\sigma_U} \exp\left(-\frac{\sqrt{Z}}{\sigma_U}\right) \mathrm{d}Z \\ &= 2\sigma_U^2. \end{aligned} \tag{17}$$

The mean-square value is

$$\begin{aligned} \mathrm{E}\left[Z^2\right] &= \int_{-\infty}^{\infty} Z^2 \Pr(Z) \mathrm{d}Z \\ &= \frac{1}{2\sigma_U} \int_{0}^{\infty} (\sqrt{Z})^3 \exp\left(-\frac{\sqrt{Z}}{\sigma_U}\right) \mathrm{d}Z \\ &= 24\sigma_U^4, \end{aligned} \tag{18}$$

giving a variance of

$$\begin{aligned} \mathrm{Var}[Z] &= \mathrm{E}\left[Z^2\right] - (\mathrm{E}[Z])^2 \\ &= 20\sigma_U^4. \end{aligned} \tag{19}$$

### *C. Unknown Pixel Statistics*

Now consider a general speckle probablity distribution, for example obtained from filtering the speckle. The mean and variance of $Z$ can be approximated as a function of the mean and variance of $U$ using the delta method. (See the Appendix.) Using (A.35), we obtain

$$\mathrm{E}[Z] \approx {\mu_U}^2 + \sigma_U^2. \tag{20}$$

This matches the negative exponential case in (17) where ${\mu_U}^2 = \sigma_U^2$. Using (A.36), we obtain

$$\mathrm{Var}[Z] \approx 4\mu_U^2 \sigma_U^2. \tag{21}$$

This approximation severely underestimates the variance in (19). An exact result can be obtained for the transform $Z = U^2$ from using 4 terms of the Taylor Series, giving

$$\mathrm{Var}[Z] = \mathrm{E}\left[U^4\right] - 2{\mu_U}^2 {\sigma_U^2}^2 - {\mu_U}^4 - {\sigma_U^2}^4. \tag{22}$$

### *D. Mean of Contrast Measure*

Let us calculate the statistics of the contrast measure $C$ in (15). As $Z$ is spatially stationary, $\mathrm{E}[Z(m,n)]$ and $\mathrm{Var}[Z(m,n)]$ are constant for all $(m,n)$, and

$$\begin{aligned} \mathrm{E}[C] &= \mathrm{E}[Z] \frac{1}{N} \sum_{(m,n)} V^2(m,n) \\ &= \mathrm{E}[Z] \widehat{C} \end{aligned} \tag{23}$$

where $\widehat{C}$ is the contrast of the noncoherent image of the object. For fully developed speckle, (17) gives

$$\mathrm{E}[C] = 2\sigma_U^2 \widehat{C}. \tag{24}$$

Fig. 6 shows the mean contrast value for a number of simulated speckle patterns as $\sigma_U^2$ is varied. The results match those predicted in (24) closely.

### *E. Variance of Contrast Measure*

The variance of $C$ is given by

$$\begin{aligned} \mathrm{Var}[C] = \mathrm{Var}[Z] \frac{1}{N^2} \sum_i V_i^4 \\ + \frac{\mathrm{Var}[Z]}{N^2} \sum \sum_{i \neq j} V_i^2 V_j^2 \, \mathrm{Corr}[Z_i, Z_j]. \end{aligned} \tag{25}$$

Thus the contrast variance depends on the speckle autocorrelation coefficient. For negative exponential pixel intensity statistics, the autocorrelation coefficient of $Z$ can be shown to be

$$\begin{aligned} \mathrm{Corr}[Z_i, Z_j] &= \frac{\mathrm{E}[Z_i Z_j] - \mathrm{E}[Z_i]\,\mathrm{E}[Z_j]}{\sqrt{\mathrm{Var}[Z_i]\,\mathrm{Var}[Z_j]}} \\ &= \frac{\rho_{ij}^4 + 4\rho_{ij}^2}{5}. \end{aligned} \tag{26}$$

In the case of uncorrelated speckle, $\rho_{ij} = 0$ and

$$\begin{aligned} \mathrm{Var}[C] &= \mathrm{Var}[Z] \frac{1}{N^2} \sum_i V_i^4 \\ &= \frac{20\sigma_U^4}{N} \widehat{K}, \end{aligned} \tag{27}$$

where

$$\widehat{K} = \frac{1}{N} \sum_i^N V_i^4.$$

This is often refered to as delta-correlated speckle [20]. No physical system can give perfectly delta-correlated speckle as it requires infinite bandwidth but it is a good approximation. Fig. 7 shows how $\mathrm{Var}[C]$ varies with $\sigma_U$ for a number of simulated uncorrelated speckle patterns. The data matches (27) closely.

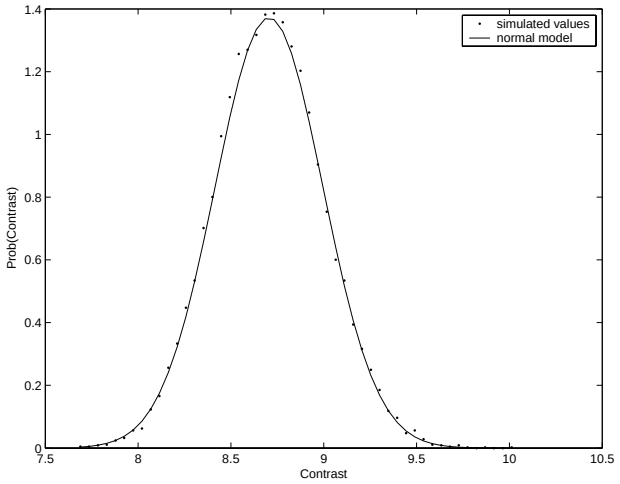


Fig. 5. Estimated probability distribution of contrast from simulated speckle. Data has mean and variance of $\mu_C$=8.7 $\sigma_C^2$=0.085 respectively. Data is compared against normal distribution model: $\Pr(C) = \frac{1}{\sqrt{2\pi\sigma_C^2}} \exp\left(-\frac{(C-\mu_C)^2}{2\sigma_C^2}\right)$.

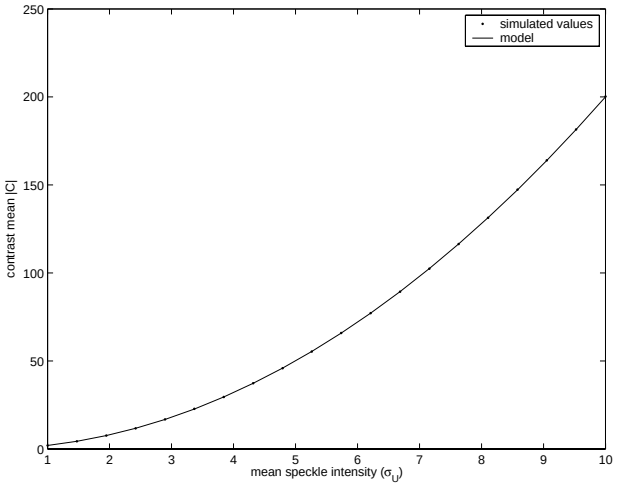


Fig. 6. The mean contrast for several speckle realisations as a function of the mean speckle intensity $\sigma_U$. It is compared against the model: $\mathrm{E}[C] = 2\sigma_U^2$.

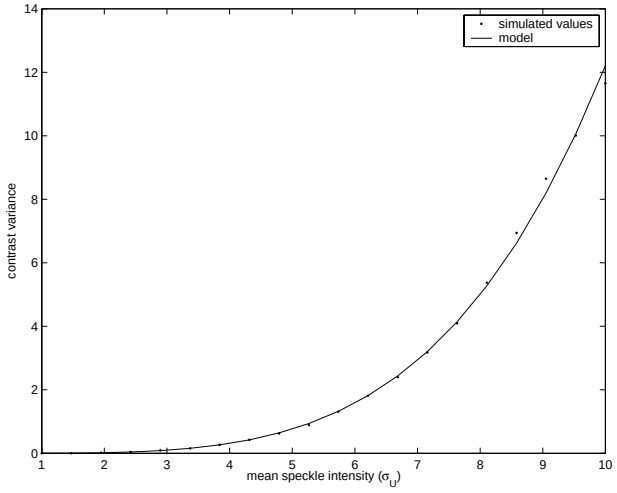


Fig. 7. The variance of the contrast for several speckle realisations as a function of the mean speckle intensity $\sigma_U$. It is compared against the model: $\mathrm{Var}[C] = 20\sigma_U^4/N$.

### *F. Distribution of Contrast Measure*

If $C$ is normally distributed, the distribution of $C$ is given by

$$\Pr(C) = \frac{1}{\sqrt{2\pi\,\mathrm{Var}[C]}} \exp\left(-\frac{(C-\mathrm{E}[C])^2}{2\,\mathrm{Var}[C]}\right). \qquad (28)$$

## V. RESULTS

A 128×128 pixel speckle image was simulated with 10000 different speckle realisations. This was repeated for a number of different speckle variances and correlation lengths of the speckle. There was a uniform background, i.e. $V(m,n) = 1$.

Fig. 5 shows an instance of a probability distribution of the contrast for uncorrelated speckle. It matches the normal distribution model well. The contrast was measured for a range of uncorrelated speckle patterns, varying the mean speckle intensity $\sigma_U$. The mean contrast value matched that predicted by (24) well as shown in Fig. 6. The variance of the same data is shown in Fig. 7. This fits the model of (27) well.

The speckle was modeled to have a Gaussian correlation. The correlation length $L_c$ is defined as the distance it takes in pixels for the correlation to drop to $1/e$. The mean speckle intensity intensity was then held constant and the correlation length $L_c$ varied. Fig. 8 shows how the probability distribution varies with speckle correlation length. The mean of the contrast measurement did not vary with correlation length. Fig. 9 shows how the variance of the contrast varies with correlation length. This shows the contrast variance increasing approximately at the rate of the square of the correlation length. This is predicted by (25) for small $\rho_{ij}$.

## VI. MAXIMISING THE CONTRAST

The probability density function derived for $C$ explains why we observe the large variation of $C$ in Fig. 2. If this was an incoherent image there would be a smoothly varying curve, with a peak at the correctly focused value. In an incoherent image, each measure of contrast $C$ is a random variable. The mean of $C$ is proportional to the incoherent case (see (23), giving the smooth curve and peak. Hiding this peak is the fact that each contrast measurement also has an associated variance caused by the speckle given by (25). Our ability to perform contrast optimisation is limited to the size of this variance, a fact ignored by most authors on the subject.

Any change in focus parameter will need to be large enough to cause a change in contrast large enough so that the two probability distribution curves do not overlap significantly. This is shown in Fig. 10. Consider making two contrast measurements, $C_1$ and $C_2$, for different focus parameters and defining the quantity

$$\delta \equiv C_2 - C_1. \qquad (29)$$

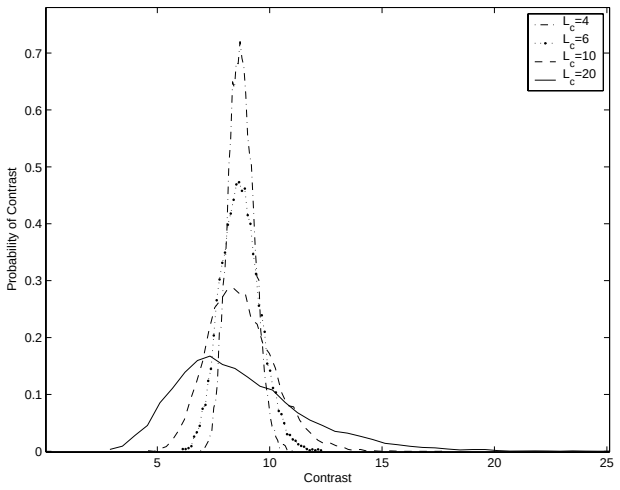


Fig. 8. Probability distributions of contrast for several simulated speckle patterns. Shown for varied correlation lengths, $L_c = 4, 6, 10, 20$.

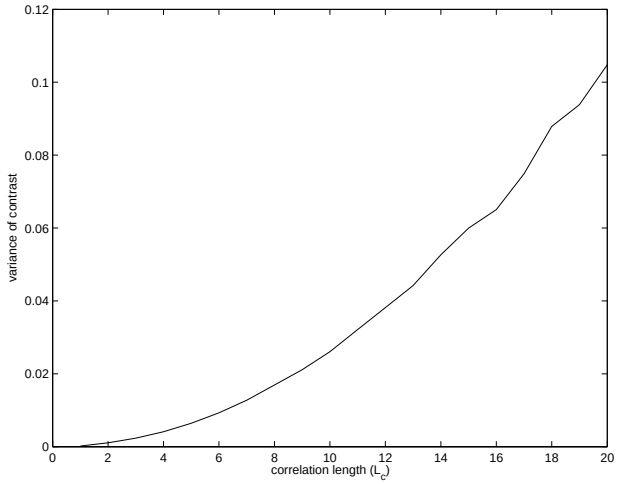


Fig. 9. Variance of contrast over several speckle patterns as a function of speckle correlation length $L_c$.

If $C$ is normally distributed, $\delta$ will also be normally distributed, with mean of

$$\mathrm{E}\left[\delta\right] = \mathrm{E}\left[C_2\right] - \mathrm{E}\left[C_1\right], \tag{30}$$

and variance

$$\mathrm{Var}\left[\delta\right] = \mathrm{Var}\left[C_2\right] + \mathrm{Var}\left[C_1\right]. \tag{31}$$

The ability to correctly distinguish a change in the contrast of an image (as opposed to speckle noise) is determined by the ratio of the mean and standard deviation of $\delta$. Assuming delta-correlated speckle and using (23) and (27), this gives

$$\begin{aligned} d &\equiv \frac{\mathrm{E}\left[\delta\right]}{\sqrt{\mathrm{Var}\left[\delta\right]}} \\ &= \frac{\mathrm{E}\left[Z\right]\left(\frac{1}{N}\sum_{(m,n)} V_2^2(m,n) - \frac{1}{N}\sum_{(m,n)} V_1^2(m,n)\right)}{\sqrt{\mathrm{Var}\left[Z\right]}\sqrt{\frac{1}{N^2}\sum_{(m,n)} V_2^4(m,n) + \frac{1}{N^2}\sum_{(m,n)} V_1^4(m,n)}}. \end{aligned} \tag{32}$$

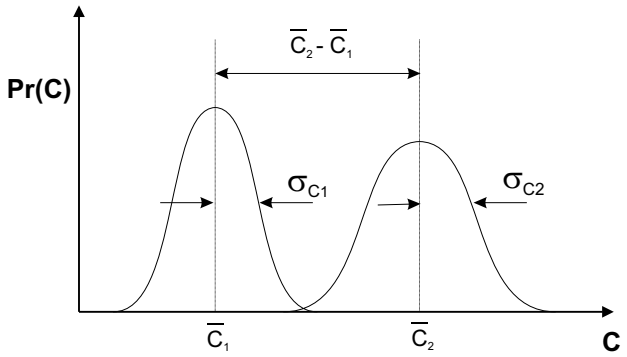


Fig. 10. Probability density function of image contrast for two different focus values.

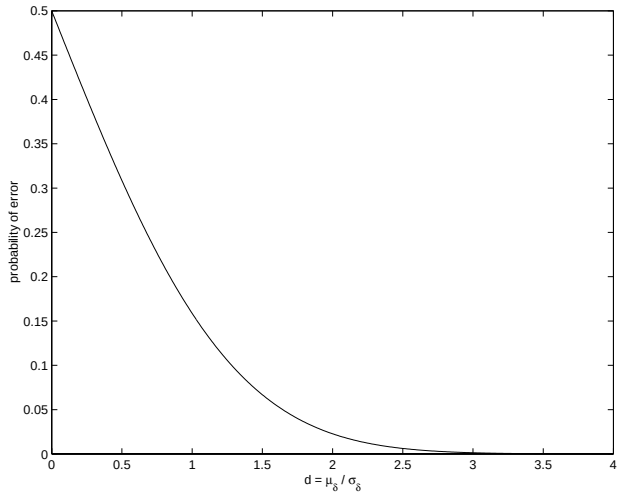


Fig. 11. Probability of correctly distinuishing two contrast values, as a function of the ratio of the mean and standard deviation of the difference between the two values.

Using (17), (19), and (27),

$$d = \frac{2}{\sqrt{20N}} \frac{\widehat{C_2} - \widehat{C_1}}{\sqrt{\widehat{K_2} + \widehat{K_1}}}. \tag{33}$$

Without loss of generality, if we assume $\mathrm{E}\left[\delta\right] > 0$, then the probability of correctly distinguishing whether $C_2 > C_1$ is given by

$$\Pr\left(\delta < 0\right) = \tfrac{1}{2}\,\mathrm{erfc}\left(\frac{d}{\sqrt{2}}\right). \tag{34}$$

If $\mathrm{E}\left[\delta\right] < 0$, then the probability of an error is $\Pr\left(0 < \delta\right)$ which gives the same result. Fig. 11 shows how the probability of an error varies with $d$. This shows the content of a scene $V$ requires $d > 2$ for a reasonable result.

## VII. CONCLUSIONS

The statistical distribution of the contrast measure of a coherent image has been developed. This is, necesarily, a function of the imaged scene, so no general conclusions on the sucess or otherwise of contrast optimisation can be made. It is clear however, that the target-speckle ratio is crucial in

determining the success of the method. The exact nature of this relationship has yet to be determined.

To improve the ability of contrast optimisation to focus coherent images $d$, the ratio of mean and standard deviation of the difference of two contrast measures must be larger than two. For SAS images from kiwiSAS III, this is not the case, thus $d$ must be increased. One way is to increase the target to speckle ratio in the image. A simple approach is to use a weighted contrast measure [13], which increases the weight of strong targets, and reduces it for speckle.

One promising improvement was to reduce the variance of the speckle with speckle-reduction techniques such as multi-look averaging [21]. This increases the mean-square to variance ratio of pixel intensity by trading off spatial resolution. Intuitively this should increase the contrast mean to standard-deviation ratio, $d$. However, experiments showed that the variance of $C$ is not reduced by multi-look speckle-reduction. The reason for this is the reduction in spatial resolution results in an increase in the variance of the contrast from the correlation term in (25).

This result illustrates the usefulness of the derived contrast statistics as a tool in understanding and improving contrast optimisation of coherent images.

## APPENDIX

Delta Method:

Let $X$ be a random variable $(-\infty < X < \infty)$, $g(X)$ be a function of $X$, $\mu = \mathrm{E}[X]$ be the mean of $X$ and $\sigma^2 = \mathrm{Var}[X]$ be the variance of X.

Then the mean and variance of the function $g(X)$ are given in terms of the mean and variance of $X$ by the following approximations [22]:

$$\mathrm{E}[g(X)] \approx g(\mu) + \tfrac{1}{2}\sigma^2 g''(\mu) \tag{A.35}$$

and

$$\mathrm{Var}[g(X)] \approx \sigma^2 [g'(\mu)]^2 \tag{A.36}$$

where

$$g'(\mu) = \left.\frac{d}{dx} g(x)\right|_{x=\mu}$$

and

$$g''(\mu) = \left.\frac{d^2}{dx^2} g(x)\right|_{x=\mu}.$$

This is known as the delta method, obtained by a one step Taylor approximation of $g(X)$ about the mean $\mu$. This is only a good approximation if $X$ has a high probability of being close to its mean $\mu$ i.e. the variance $\sigma^2$ is small.

## ACKNOWLEDGMENTS

The authors would like to thank Dr Peter J. Smith of the Department of Electrical and Computer Engineering, University of Canterbury for developing the second-order statistics of the contrast measure, plus many useful discussions.

## REFERENCES

[1] L. Nock, G. Trahey, and S. Smith, "Phase aberration correction in medical ultrasound using speckle brightness as a quality factor," *Journal of the Acoustics Society of America*, vol. 85, pp. 1819–1833, May 1989.

[2] E. H. Attia and B. Steinberg, "Self-cohering large antenna arrays using the spatial correlation properties of radar clutter," *IEEE Transactions on Antennas and Propagation*, vol. 37, pp. 30–38, January 1989.

[3] J. C. Curlander and R. N. McDonough, *Synthetic Aperture Radar: Systems and signal processing*. New York: John Wiley and sons, 1996.

[4] P. T. Gough and D. W. Hawkins, "Imaging algorithms for a strip-map synthetic aperture sonar: Minimizing the effects of aperture errors and aperture undersampling," *IEEE Journal of Oceanic Engineering*, vol. 22, pp. 27–39, January 1997.

[5] R. A. Muller and A. Buffington, "Real-time correction of atmospherically degraded telescope images through image sharpening," *Journal of the Optical Society of America*, vol. 64, pp. 1200–1210, September 1974.

[6] R. G. Paxman and J. C. Marron, "Abberation correction of speckled imagery with an image-sharpness criterion," in *Proceedings of SPIE*, vol. 976, pp. 37–47, 1988.

[7] D. Blacknell, A. P. Blake, C. J. Oliver, and R. G. White, "A comparison of SAR multilook registration and contrast optimisation autofocus alogrithms applied to real SAR data," in *International Radar Conference*, pp. 363–366, 1992.

[8] F. Berizzi and G. Corsini, "Autofocusing of inverse synthetic aperture radar images using contrast optimization," *IEEE Transactions on Aerospace and Electronic Systems*, vol. 32, pp. 1185–1191, July 1996.

[9] F. Berizzi, G. Corsini, M. Diani, and M. Veltroni, "Autofocus of wide azimuth angle SAR images by contrast optimisation," in *International Geoscience and Remote Sensing Symposium Proceedings*, vol. 2, pp. 1230–1232, 1996.

[10] L. Xi, L. Guosui, and J. Ni, "Autofocusing of ISAR images based on entropy minimization," *IEEE Transactions on Aerospace and Electronic Systems*, vol. 35, pp. 1240–1252, October 1999.

[11] P. T. Gough and R. G. Lane, "Autofocussing SAR and SAS images using a conjugate gradient search alogirithm," in *Geoscience and Remote Sensing Symposium Proceedings, 1998*, vol. 2, pp. 621–623, IEEE, 1998.

[12] J. Fienup, "Synthetic-aperture radar autofocus by maximizing sharpness," *Optics Letters*, vol. 25, pp. 221–223, February 15 2000.

[13] J. R. Fienup and J. J. Miller, "abberation correction by maximising generalized sharpness metrics," *Journal of the Optical Society of America A*, vol. 20, pp. 609–620, April 2003.

[14] T. J. Sutton, S. A. Chapman, and H. D. Griffiths, "Robustness and effectiveness of autofocus algorithms applied to diverse seabed environments," in *Proceedings of the fifth European Conference on Underwater Acoustics ECUA 2000* (M. E. Zakharia, ed.), vol. 1, pp. 407–412, EUCA, July 2000.

[15] S. A. Fortune, M. P. Hayes, and P. T. Gough, "Statistical autofocus of synthetic aperture sonar images using image contrast optimisation," in *OCEANS 2001*, vol. 1, pp. 163–169, IEEE, November 2001.

[16] J. A. Nelder and R. Mead, "A simplex method for function minimisation," *Computer Journal*, vol. 7, no. 4, pp. 308–313, 1965.

[17] J. W. Goodman, "Statistical properties of laser speckle patterns," in *Laser speckle and related phenomena* (J. C. Dainty, ed.), pp. 9–75, Springer-Verlag, Berlin, 1975.

[18] S. Lowenthal and H. Arsenault, "Image formation for coherent diffuse objects: Statistical properties," *Journal of the Optical Society of America*, vol. 60, pp. 1478–1483, November 1970.

[19] H. White, *Asymptotic Theory for Econometricians*. Academic Press, 1984.

[20] J. Marron and G. M. Morris, "Image recognition in the presence of laser speckle," *Journal of the Optical Society of America*, vol. 3, pp. 964–971, 1986.

[21] S. A. Fortune, M. P. Hayes, and P. T. Gough, "Speckle reduction of synthetic aperture sonar images," in *World Conference on Ultrasonics, Paris, September 2003*, 2003.

[22] D. Blumenfeld, *Operations Researcg Calculations Handbook*. CRC Press, 2001.